

Nuclear and atomic moments and hyperfine-structure parameters of ^{253}Es and $^{254m}\text{Es}^\dagger$

L. S. Goodman, H. Diamond, and H. E. Stanton

Argonne National Laboratory, Argonne, Illinois 60439

(Received 10 October 1974)

The atomic-beam magnetic-resonance method has been used to study atoms of the isotopes ^{253}Es and ^{254m}Es . The parameters of the Hamiltonian which fit the experimental data for ^{253}Es are $I = 7/2$, $J = 15/2$, $A = 817.153(7)$ MHz, $B = -4316.254(76)$ MHz, $\mu_I = 4.10(7)\mu_N$, and $g_J = 1.185138(5)$. The spectroscopic nuclear electric quadrupole moment calculated from the B factor is $Q_S = 6.9(8)$ b. For ^{254m}Es the parameters $I = 2$, $A = 1020(12)$ MHz, and $B = -2387(160)$ MHz fit the data. The magnetic dipole moment and electric quadrupole moment inferred from these values are $\mu_I = 2.90(7)\mu_N$ and $Q_S = 3.8(5)$ b. The high precision of the Landé g -value determination was used to calculate an atomic ground-state eigenvector. For ^{253}Es the ratio of the measured A factor to the nuclear magnetic moment agrees well with the calculations of Lewis *et al.*

INTRODUCTION

Along with the nuclear spin I and the electronic angular momentum J , the atomic-beam magnetic-resonance technique can provide high-precision determinations of electron g factors and hyperfine interaction constants, and the direct determination of nuclear magnetic dipole moments. Such information can be very useful in guiding theoretical investigations of atomic states and their interactions, and especially in checking the adequacy of numerical *ab initio* calculations of atomic parameters.

The extension of this technique to the study of einsteinium yields the values of atomic parameters near the extreme limits of nuclear mass and charge available in the laboratory, and challenges atomic theory in a region where relativistic effects should be very important; it also provides data that is of potential value to the further development of nuclear theory for this region.

I. EXPERIMENTAL DETAILS

The method used in the present study was the classic atomic-beam magnetic-resonance technique of Rabi *et al.* and Zacharias¹ as adapted for experiments with radioactive isotopes.²

The source oven was made of tantalum metal and was equipped with an inner, sharp-lipped, tantalum crucible in which the experimental charge was loaded. Each loading required a few micrograms of einsteinium and about 3 mg of samarium carrier coprecipitated as hydroxide and heated in air to the sesquioxide. A few pieces of lanthanum alloy (10 wt% aluminum to retard oxidation in air³) in stoichiometric excess were added to reduce the oxide and produce neutral einsteinium atoms in the beam. A small amount of potassium chloride was placed below the inner crucible, out of contact with the rare-earth mixture, to form a beam

of atoms which could be detected with a surface-ionization detector and which could be used to align and position the oven slit for optimum transmission of an undeflected beam through the apparatus.

The collector planchets were made of $0.5 \times 1 \times 0.03$ -in. soft steel. They were cleaned and given a rough surface by tumbling them in a slurry of sand in methyl alcohol. This treatment provided collectors of uniform efficiency as can be observed from the uniformity of background counts in the resonance shown in Fig. 1.

It was found empirically that if an exposure of a collector to the open or undeflected beam for 1 min yielded a counting rate of 100 counts/min, the counting rate at resonance would be sufficient to attain an adequate signal-to-noise ratio. It was easy to obtain such a counting rate, but the beam intensity declined rather rapidly with time, however, and after an hour or so was only a few counts per minute. It could be increased by applying more heat to the oven but could not be made steady enough to take data in the usual fashion.² A new collector system was designed so that interpretable data could be collected in the face of this difficulty.

Twenty collectors were mounted on a spindle (Fig. 2) so that they could be rotated sequentially once per second behind the collector slit. The applied radio frequency was changed stepwise repeatedly in synchronism with the collectors. This rapid, repetitive, sequential sampling technique allows each collector to be exposed to the same average beam source and obviates the need for steady oven conditions. That this beam-source averaging technique is effective is apparent from the uniformity of the background counts off the resonance shown in Fig. 1.

Although it was impossible to predict the exact

counting rate that would be attained, an exposure of 1 to 2 h, during which period the power for heating the oven was increased a few times, would usually yield a counting rate at the center of the resonance of 0.5–3 counts/min with a signal-to-background ratio between 1.3 and 3. The 2π α -particle proportional counters all had background counting rates of less than 0.1 count/min which could be subtracted reliably. An overnight count yielded data of which Fig. 1 is a sample. A single oven loading was sufficient for as many as a dozen resonance searches.

The required uniform magnetic field was set and held by means of a resonance (for which the radio-frequency power was applied throughout the run with the same rf loop as for the search frequency) of either potassium or cesium atoms in a beam from an auxiliary oven. An electronic circuit which processed the signal produced by the alkali beam automatically held the C field close to its assigned value. The quality of the data was greatly enhanced by the use of this device.

II. ^{253}Es EXPERIMENT

A few resonances at low magnetic field established the values of the atomic angular momentum of the ground state $J = \frac{15}{2}$ and the nuclear spin $I = \frac{7}{2}$ which confirm the values obtained by optical spectroscopy⁴ and decay schemes.⁵ The resonance frequencies found are listed in Table I along with their associated magnetic fields. The four fundamental parameters of the Hamiltonian⁶

$$\mathcal{H} = A\vec{I} \cdot \vec{J} + BQ_{op} + g_J \mu_B \vec{J} \cdot \vec{H} + g_I \mu_N \vec{I} \cdot \vec{H}, \quad (1)$$

A , B , g_J , and g_I , were varied to obtain a least-squares (l.s.) fit to these data. The difference

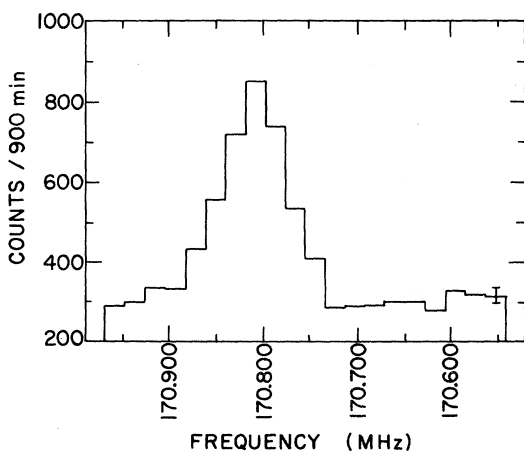


FIG. 1. Experimental resonance curve for the ^{253}Es ($F=4$, $m_F=4 \leftrightarrow F=4$, $m_F=3$) transition at 60 G.

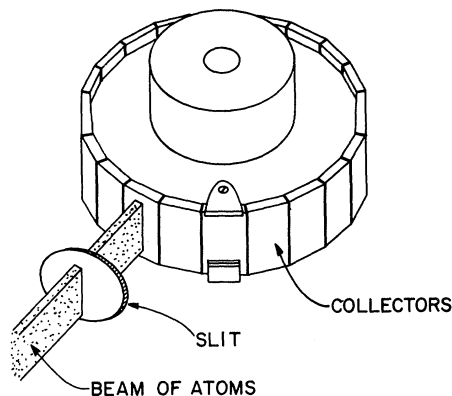


FIG. 2. Arrangement for exposing 20 collectors sequentially and repetitively. The radio frequency used to induce transitions is synchronously stepped in coordination with the collectors.

between the frequency derived by the fitting program⁷ and the observed frequency ($\Delta = \nu_{\text{obs}} - \nu_{\text{l.s.}}$) is listed in column 4 of Table I. The parameters which fit the data best are listed in Table II along with the calculated goodness-of-fit parameter χ^2 .

Interpretation of the data

The value of $g_J = 1.185138(5)$ is much smaller than 1.198464, which would be expected from a

TABLE I. Observed transitions for ^{253}Es .

$F, m_F \leftrightarrow F' m'_F$	H (G)	Frequency (MHz)	$\Delta = \nu_{\text{obs}} - \nu_{\text{l.s.}}$ (kHz)
11, -3 \leftrightarrow 11, -4	40.000(5)	45.276(20)	5
11, -3 \leftrightarrow 11, -4	80.000(5)	90.621(20)	-5
4, 4 \leftrightarrow 4, 3	30.000(5)	85.009(20)	3
4, 4 \leftrightarrow 4, 3	40.000(5)	113.500(20)	-14
4, 4 \leftrightarrow 4, 3	60.000(5)	170.799(10)	3
11, -3 \leftrightarrow 11, -4	200.000(5)	227.200(20)	-8
4, 4 \leftrightarrow 4, 3	100.000(5)	286.432(15)	2
4, 4 \leftrightarrow 4, 3	200.000(5)	581.889(20)	-24
7, 1 \leftrightarrow 7, 0	400.000(5)	616.140(10)	15
11, -3 \leftrightarrow 11, -4	400.000(2)	456.620(5)	0
9, -1 \leftrightarrow 9, -2	400.000(2)	512.160(10)	-5
4, 4 \leftrightarrow 4, 3	400.000(2)	1200.590(20)	-19
5, 3 \leftrightarrow 5, 2	400.000(2)	856.970(20)	7
4, 4 \leftrightarrow 4, 3	600.000(2)	1851.165(15)	-50
4, 4 \leftrightarrow 4, 3	765.431(3)	2399.976(30)	-32
5, 3 \leftrightarrow 5, 2	1081.819(3)	2400.090(18)	-30
4, 4 \leftrightarrow 4, 3	1000.040(3)	3154.734(12)	23
4, 4 \leftrightarrow 4, 3	1140.000(2)	3572.196(20)	50
4, 4 \leftrightarrow 4, 3	1300.000(2)	4012.118(20)	-20
5, 3 \leftrightarrow 5, 2	1740.000(2)	4016.727(30)	-1
6, 2 \leftrightarrow 6, 1	2000.000(4)	3790.116(60)	94
5, 3 \leftrightarrow 4, 3	1500.000(5)	4814.910(30)	16
5, 3 \leftrightarrow 4, 3	10.000(2)	4858.660(10)	-10
6, 2 \leftrightarrow 5, 2	15.000(2)	5649.188(20)	40
7, 1 \leftrightarrow 6, 1	15.000(2)	6333.125(20)	-7
8, 0 \leftrightarrow 7, 0	15.000(2)	6889.558(5)	0

pure ${}^4I_{15/2}$ state with Schwinger, relativistic, and diamagnetic corrections included. This difference must be ascribed to mixing from other states of the same J . In the $f^{11}s^2$ configuration the only state that would be expected to contribute substantially to the ground state is the ${}^2K_{15/2}$ state which is $23\,000\text{ cm}^{-1}$ higher.⁸ The next $J_{15/2}$ state, the ${}^2L_{15/2}$, is not only considerably higher in energy at $43\,000\text{ cm}^{-1}$ above the ground state (GS),⁸ but also differs in the total orbital angular momentum L by $2\hbar$. It can thus influence the ground state only indirectly. The present accuracy of theoretical and empirical eigenvectors is not high enough to warrant anything beyond the use of a two-state model:

$$\psi_{\text{GS}} = (1 - \eta^2)^{1/2} |{}^4I_{15/2}\rangle + \eta |{}^2K_{15/2}\rangle. \quad (2)$$

This leads to the equation

$$g_J = (1 - \eta^2)(1.200\,464) + \eta^2(1.066\,821) - 0.002, \quad (3)$$

where the numbers in parentheses are the L - S values of g_J with Schwinger correction for ${}^4I_{15/2}$ and ${}^2K_{15/2}$, respectively, and the number 0.002 is a relativistic and diamagnetic correction, the estimate of which seems reasonable from measurements and calculations on the g_J of fermium.⁹ The solution of Eq. (3) with g_J assigned the experimental value is $|\eta| = 0.3158$. That $\eta = -0.3158$ follows from elementary perturbation theory and the fact that the spin-orbit matrix element between the two states is positive.

Once the value of η and thus the eigenvector (2) is known, we can calculate the necessary matrix elements¹⁰ for the nuclear magnetic dipole and electric quadrupole hyperfine interactions. The hyperfine-interaction constants A and B can thereby be expressed in terms of the Sandars and Beck parameters, which have in turn been expressed^{10, 11} in terms of relativistic radial integrals and the static moments of the nucleus. These radial integrals for einsteinium have been calculated numerically with relativistic, self-consistent, Dirac-Slater wave functions by Lewis *et al.*¹² The details of the treatment which uses these integrals is presented in the Appendix.¹³

For the present suffice it to say that with this treatment the nuclear magnetic dipole moment can be calculated from the A factor in Table II. The value thus derived is $\mu(A) = 4.08\mu_N$. This should be compared to the direct value obtained by fitting the parameters of the Hamiltonian to the resonance data, $\mu_{\text{dir}} = 4.10(7)\mu_N$.

The excellence of this agreement is admittedly fortuitous. The two-component eigenvector is an approximation that should allow only modest claims of accuracy. Lewis *et al.*, though they should be rightfully pleased with the agreement,

make no claims for such high precision.

These caveats aside, the agreement is encouraging enough so that we are inclined to trust the eigenvector and the calculations of Lewis *et al.* to the extent of using them to estimate the nuclear electronic quadrupole moment from the B factor in Table II. The details of this calculation are in the Appendix.

We find that the B factor in Table II corresponds to a nuclear electric quadrupole moment $Q_u = 6.01$ b. This value is still uncorrected for Sternheimer shielding,¹⁴ which has not been calculated. Sternheimer has been willing to venture an educated guess¹⁵ based on his knowledge of the shielding for the $4f$ shell. Because the $5f$ shell is so largely filled for einsteinium, the sign of R is almost undoubtedly positive. Its value is probably within the range $R = 0.1 \pm 0.1$, where the value of the quadrupole moment with Sternheimer shielding taken into account, Q_s , is related to the uncorrected value Q_u by the relation

$$Q_s = Q_u (1/(1 - R)). \quad (4)$$

The best estimate of the spectroscopic quadrupole moment of ${}^{253}\text{Es}$ is then

$$Q_s = 6.7(8) \text{ b.}$$

III. ${}^{254m}\text{Es}$ EXPERIMENT

The details of the ${}^{254m}\text{Es}$ experiment were in the main the same as those for ${}^{253}\text{Es}$. There were, however, a few important differences. The 39-h ${}^{254m}\text{Es}$ decays by β^- emission to 3.2-h ${}^{254}\text{Fm}$; the fermium in turn decays by α emission. Because the α counters have intrinsic backgrounds which are 50–100 times lower than those of our β counters, we decided to count the fermium- α decays as a measure of the ${}^{254m}\text{Es}$ which condensed on the collectors.

The ${}^{254m}\text{Es}$ was produced by neutron capture on ${}^{253}\text{Es}$ in the HFIR rabbit at the Oak Ridge National Laboratory. Each sample was irradiated for approximately 1.7 days in a flux of $(3\text{--}5) \times 10^{15}$ neutrons/cm² sec.

The resultant einsteinium samples were thus not

TABLE II. Hamiltonian parameters that provide the best fit to the data of Table I. The quoted errors are standard deviations given by the least-squares fitting program. (See Ref. 7.)

A (MHz)	B (MHz)	g_J	μ_I	χ^2
817.1495(12)	-4316.254(76)	1.185 138(5)	4.10(7) μ_N	33 ^a

^a 26 data and four parameters.

isotopically pure, and the signal-to-background ratio was reduced from that of the ^{253}Es experiment to values of 1.06–1.5. Figure 3 shows one of the better resonances found in the ^{254m}Es experiment. Table III lists the resonance frequencies and associated magnetic fields.

The only value of nuclear spin which allows a fit to the data is $I = 2$. The value inferred from nuclear and β -decay systematics is in agreement with this determination.¹⁶

In order to find the parameters of the Hamiltonian that give the best prediction of these data, only the A and B factors were allowed to vary in the fitting program; g_J was held equal to the value 1.185 138 obtained in the ^{253}Es experiment, and the nuclear gyromagnetic ratio was constrained to be $g_I(254m) = g_I(253)A(254m)/A(253)$.

The best values of the Hamiltonian parameters and the static moments inferred from the A and B factors for both ^{253}Es and ^{254m}Es can be found in Table IV. Errors are stated in standard deviations.

IV. NUCLEAR MOMENTS

^{253}Es

The magnetic moment of odd- A deformed nuclei can be calculated from the wave functions of Nilsson.¹⁷ Lamm,¹⁸ using an improved Nilsson-model Hamiltonian has calculated the ^{253}Es magnetic moment to be $4.24\mu_N$ if g_s for the proton is taken to be the free proton value 5.59, or $3.65\mu_N$ if g_s is taken to be 0.6 that of the free proton value.¹⁹ These calculated values can be compared to our experimental value $4.10(7)\mu_N$ shown in Table II. Other measurements of the magnetic moment of

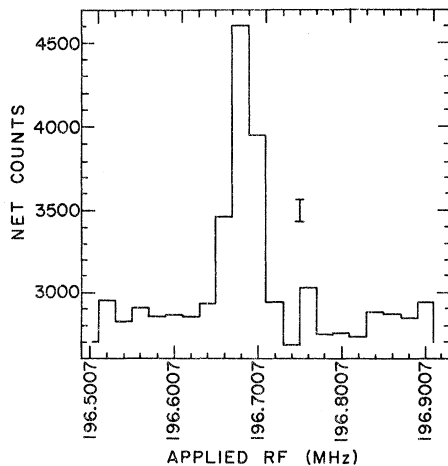


FIG. 3. Experimental resonance curve for the ^{254m}Es ($F = \frac{11}{2}, m_F = -\frac{3}{2} \leftrightarrow F = \frac{11}{2}, m_F = -\frac{5}{2}$) transition at 400 G.

TABLE III. Transitions observed for ^{254m}Es .

$F, m_F \leftrightarrow F', m_F'$	H (G)	Frequency (MHz)	$\Delta = \nu_{\text{obs}} - \nu_{\text{ls}}$ (kHz)
$\frac{11}{2}, \frac{5}{2} \leftrightarrow \frac{11}{2}, \frac{3}{2}$	50.000(3)	108.566(8)	-13
$\frac{11}{2}, \frac{5}{2} \leftrightarrow \frac{11}{2}, \frac{3}{2}$	100.000(3)	217.354(8)	-1
$\frac{11}{2}, \frac{5}{2} \leftrightarrow \frac{11}{2}, \frac{3}{2}$	150.000(3)	326.338(12)	24
$\frac{11}{2}, \frac{5}{2} \leftrightarrow \frac{11}{2}, \frac{3}{2}$	200.000(3)	435.438(10)	-7
$\frac{13}{2}, \frac{3}{2} \leftrightarrow \frac{13}{2}, \frac{1}{2}$	50.000(3)	90.583(30)	-14
$\frac{13}{2}, \frac{3}{2} \leftrightarrow \frac{13}{2}, \frac{1}{2}$	600.000(3)	1087.707(30)	-1
$\frac{15}{2}, \frac{1}{2} \leftrightarrow \frac{15}{2}, -\frac{1}{2}$	600.000(3)	949.784(20)	-7
$\frac{15}{2}, \frac{1}{2} \leftrightarrow \frac{15}{2}, -\frac{1}{2}$	400.000(3)	632.691(7)	3
$\frac{19}{2}, \frac{3}{2} \leftrightarrow \frac{19}{2}, -\frac{5}{2}$	150.000(3)	196.683(6)	3
$\frac{13}{2}, \frac{3}{2} \leftrightarrow \frac{13}{2}, \frac{1}{2}$	400.000(3)	724.790(25)	-47

^{253}Es give $(3.6 \pm 0.4)\mu_N$ from optical spectra,⁴ $(3.6 \pm 0.5)\mu_N$ from electron-spin-resonance measurements,²⁰ and $(2.7 \pm 1.3)\mu_N$ from anisotropic emission by aligned nuclei.²¹

The measured spectroscopic quadrupole moment Q_s is related to the intrinsic quadrupole moment Q_0 by [Ref. 16, Eq. (17)]

$$Q_s = Q_0 \frac{3K^2 - I(I+1)}{(I+1)(2I+3)}. \quad (5)$$

Both the spin (I) and its projection on the symmetry axis (K) are $\frac{7}{2}$ for the ^{253}Es ground state. The intrinsic quadrupole moment of ^{253}Es obtained from our measurements is $14.3(17)$ b.

Optical spectroscopic measurements⁴ of ^{253}Es have provided a measure of the quadrupole-inter-

TABLE IV. The values of the Hamiltonian parameters that best fit the observed resonance frequencies for ^{253}Es and ^{254m}Es along with the static moments inferred from the respective A and B factors and the calculations of Lewis *et al.*

	^{253}Es	^{254m}Es
A (MHz)	817.153(7)	1020(12)
B (MHz)	-4316.254(76)	-2387(160)
μ direct	$4.10(7)\mu_N$	
μ inferred	$4.08\mu_N$	$2.90(7)\mu_N$
Q_u^a (b)	6.01	3.32(23)
Q_s^b (b)	6.7(8)	3.7(5)
Q_0^c (b)	14.3(17)	12.9(16)
I	3.5	2
J	7.5	
g_J	1.185 138(5)	

^aSpectroscopic quadrupole moment uncorrected for Sternheimer shielding.

^bSpectroscopic quadrupole moment.

^cIntrinsic quadrupole moment.

action constant B that is much less precise but in agreement (within 30%) with the value in Table II. The intrinsic quadrupole moment of neighboring odd- A and even-even deformed nuclei may be expected to be similar; the Q_0 for ^{252}Cf has been measured at 12.9 b by Coulomb excitation.²²

An approximate intrinsic quadrupole moment may be calculated²³ from

$$Q_0 = \frac{4}{5} \epsilon Z R^2 (1 + \epsilon/2 + \frac{4}{3} \epsilon^2 - 0.302 \epsilon^3 \dots),$$

where the nuclear radius R is $1.2 A^{1/3}$ fm, Z is the nuclear charge (99), and ϵ is the deformation parameter taken (from Lamm¹⁸) to be 0.231 for ^{253}Es . This gives a calculated value for Q_0 of 12.0 b.

^{254m}Es

The uncorrected spectroscopic quadrupole moment of ^{254m}Es obtained from the B value in Table IV is $Q_u = 3.32(23)$ b; applying the Sternheimer correction of Eq. (4), the spectroscopic quadrupole moment is $Q_s = 3.7(5)$ b; from Eq. (5) the intrinsic quadrupole moment is $Q_0 = 12.9(16)$ b. This too is in good agreement with the calculated quadrupole moment, and measured intrinsic quadrupole moments of neighboring nuclei. The ratio of intrinsic quadrupole moments of ^{254m}Es and ^{253}Es can be obtained with precision since both isotopes encounter the same electronic structure and both have the same Sternheimer correction:

$$\begin{aligned} \frac{Q_0^{254m}}{Q_0^{253}} &= \frac{-(2387 \pm 160)}{-4316.25} \frac{7/2}{15/7} \\ &= 0.90(7). \end{aligned}$$

From this we can extract an estimate of the deformation parameter for ^{254m}Es (it is $\epsilon = 0.21$), and use it to calculate the magnetic moment of the odd-odd nuclide ^{254m}Es .

Hooke²⁴ has shown that the magnetic moment of an odd-odd nucleus is calculable from a model in which the odd neutron and odd proton are each coupled to the core, but do not interact appreciably with each other:

$$\mu_{\text{odd-odd}} = \frac{I}{I+1} [g_{sp} \langle S_{p3} \rangle + g_{sn} \langle S_{n3} \rangle + g_l \langle l_{p3} \rangle + g_R], \quad (6)$$

where g_R , g_{sp} , g_{sn} , and g_l , the gyromagnetic ratios for the core, proton, and neutron spins (allowing a factor of 0.6 for spin polarization), and the proton orbital angular momentum were taken to be 0.39, 3.35, -2.30, and 1, respectively. The expectation values for the spin and angular momentum operators $\langle S_{p3} \rangle$, $\langle S_{n3} \rangle$, and $\langle l_{p3} \rangle$, obtained from the tables of Browne and Femenia²⁵ at a de-

formation of $\beta = 0.22$ (equivalent to $\epsilon = 0.21$), are 0.3446, -0.2139, and 3.155.

The resultant calculated magnetic moment for the ^{254m}Es ground state $^{16} [n[622]_{\frac{3}{2}^+}; p[633]_{\frac{7}{2}^+}] 2^+$ is $3.46 \mu_N$. This rises to $4.19 \mu_N$ if g_{sn} and g_{sp} are taken to be those of the free neutron and proton. The experimental value in Table IV is $2.87(6) \mu_N$. Chen²⁶ has compared calculated and experimental magnetic moments for deformed odd-odd nuclei, and finds that a difference greater than $0.5 \mu_N$ is not unusual.

ACKNOWLEDGMENTS

R. K. Sjoblom repeatedly purified the neutron irradiated einsteinium for us. A. J. Soinski, I. Ahmad, and R. Chasman provided valuable discussions. We are grateful to W. J. Childs, M. S. Fred, R. M. Sternheimer, and M. W. Chen for their contributions (discussed in the paper).

APPENDIX

The Hamiltonian for the magnetic dipole contribution to the hyperfine interaction can be written for a single unfilled shell $(nl)^N$ in terms of Sandars-Beck¹¹ effective operators as

$$H_{\text{hfs}}(M1) = h \sum_{i=1}^N [a^{01} \vec{1}_i - (10)^{1/2} a^{12} [\vec{s} \vec{C}^{(2)}]_i^{(1)} + a^{10} \vec{s}_i] \cdot \vec{I}. \quad (A1)$$

The values of the parameters a^{ij} have been derived by Sandars and Beck in terms of integrals of relativistic radial wave functions:

$$a^{01} = D(2l+1)^{-2} [2l(l+1)F_{++} + 2l(l+1)F_{--} + F_{+-}], \quad (A2a)$$

$$\begin{aligned} a^{12} = \frac{1}{3} D(2l+1)^{-2} [&-4l(l+1)(2l-1)F_{++} \\ &+ 4l(l+1)(2l+3)F_{--} \\ &- (2l+3)(2l-1)F_{+-}], \end{aligned} \quad (A2b)$$

$$a^{10} = \frac{4}{3} D l(l+1)(2l+1)^{-2} [(l+1)F_{++} - lF_{--} - F_{+-}], \quad (A2c)$$

where $D = (2\mu_B \mu_N / h)(\mu_I / I) a_0^{-3}$ and

$$\begin{aligned} F_{jj'} = &-2[\alpha a_0 (K_j + K_{j'} + 2)]^{-1} \\ &\times \int_0^\infty (P_j Q_{j'} + Q_j P_{j'}) r^{-2} dr \end{aligned} \quad (A3)$$

are the required radial integrals.

For the integrals, P_j and Q_j refer to the large and small components of the Dirac wave function, respectively, α and a_0 are the fine-structure constant and the Bohr radius, respectively, and

$$K_j = \pm(j + \frac{1}{2}) \text{ for } l = j \pm \frac{1}{2}.$$

The radial integrals, and thus the a^{ij} , are the same for all atomic states within any given configuration. Because of the particular way in which Sandars and Beck formulated the expression (A3) in the nonrelativistic limit $F_{ij} \rightarrow \langle r^{-3} \rangle_{nl}$, $a^{01} \rightarrow a_{nl}$, $a^{12} \rightarrow a_{nl}$, and $a^{10} \rightarrow 0$, where

$$a_{nl} = (2\mu_B \mu_N / \hbar) \langle \mu_I / I \rangle \langle r^{-3} \rangle_{nl}.$$

The matrix element

$$\begin{aligned} \langle l^N S L J I F M | \mathcal{H}_{\text{nl}}(M1) | l^N S' L' J' I F M \rangle \\ = \tilde{M} \cdot \vec{J} A(l^N S L J, l^N S' L' J), \end{aligned}$$

where the $A(\psi, \psi')$ is given by Eq. (70) of Childs.¹⁰ This is the same A factor that appears in the Hamiltonian (1). For

$$\begin{aligned} \psi = |f^{11} {}^4I_{15/2}\rangle \\ = (1 - \eta^2)^{1/2} |f^{11} {}^4I_{15/2}\rangle + \eta |f^{11} {}^2K_{15/2}\rangle \end{aligned}$$

direct substitution into the expression for

$$\begin{aligned} A(\psi, \psi') = (1 - \eta^2) A({}^4I_{15/2}, {}^4I_{15/2}) + \eta^2 A({}^2K_{15/2}, {}^2K_{15/2}) \\ + 2\eta(1 - \eta^2)^{1/2} A({}^4I_{15/2}, {}^2K_{15/2}) \end{aligned} \quad (\text{A4})$$

yields

$$\begin{aligned} A({}^4I'_{15/2}) = (1 - \eta^2) \left[\frac{4}{5} a^{01} - \frac{4}{225} a^{12} + \frac{1}{5} a^{10} \right] \\ + \eta^2 \left[\frac{14}{15} a^{01} - \frac{4}{225} a^{12} + \frac{1}{15} a^{10} \right] \\ + 2\eta(1 - \eta^2)^{1/2} \left(\frac{1}{15} a^{12} \right). \end{aligned} \quad (\text{A5})$$

Lewis very kindly supplied calculations of the $F_{jj'}$, based on his self-consistent relativistic Dirac-Slater wave functions.²⁷ The values are (essentially the same for point- and finite-nucleus models) $F_{++} = 9.690$, $F_{--} = 10.698$, and $F_{+-} = 10.021$.

When these values and the previously determined value $\eta = -0.3158$ are substituted into the Eqs. (A2), and Eq. (A5) is then evaluated in terms of the a^{ij} , the result for ${}^{253}\text{Es}$ is $A({}^4I'_{15/2}) = 200.6\mu_I$ MHz, where μ_I is measured in nuclear magnetons.

An analogous Sandars-Beck effective operator equation for the contribution of the electric quadrupole interaction to the hyperfine-structure Hamiltonian is given by Childs.¹⁰ The radial integrals b^{ij} (analogous to the a^{ij} above) which are used to parametrize the Hamiltonian are given in terms of radial integrals over relativistic wave functions which are appropriate for the quadrupole interaction,

$$R_{jj'} = \int_0^\infty [P_j P_{j'} + Q_j Q_{j'}] r^{-3} dr.$$

The $R_{jj'}$ approach $\langle r^{-3} \rangle_{nl}$ in the nonrelativistic limit. Lewis has also supplied values of the $R_{jj'}$.²⁷ There is again negligible difference between corresponding values calculated for point-nucleus and finite-nucleus models. The average values are $R_{++} = 9.8105$, $R_{--} = 11.10$, $R_{+-} = 10.19$. The B factor inferred from these values is $B = -718Q$ MHz where Q is the nuclear electric quadrupole moment in barns.

†Work performed under the auspices of the U. S. Atomic Energy Commission.

¹I. I. Rabi, J. R. Zacharias, S. Millman, and P. Kusch, Phys. Rev. **53**, 318 (1938); J. R. Zacharias, Phys. Rev. **61**, 270 (1942).

²L. S. Goodman and S. Wexler, Phys. Rev. **99**, 192 (1955).

³Purchased from Ronson Metals Corp., Newark, N. J.

⁴E. F. Worden, R. W. Lougheed, R. G. Gutmacher, and J. G. Conway, J. Opt. Soc. Am. **64**, 77 (1974), and references therein.

⁵Reviewed by *The Nuclear Properties of the Heavy Elements* (Prentice-Hall, Englewood Cliffs, N. J., 1964), Vol. 2, p. 950.

⁶N. F. Ramsey, *Molecular Beams* (Oxford U. P., Oxford, England, 1956).

⁷The program HYPERFINE 4-94, written by D. H. Zurlinden of the University of California, Lawrence Radiation Laboratory, was adapted for use with the IBM-360 system at ANL.

⁸M. S. Fred (private communication).

⁹L. S. Goodman, H. Diamond, H. E. Stanton, and M. S. Fred, Phys. Rev. A **4**, 473 (1971).

¹⁰W. J. Childs, *Case Studies in Atomic Physics* (North-Holland, Amsterdam, 1973), Vol. 3, No. 4.

¹¹P. G. H. Sandars and J. Beck, Proc. R. Soc. A **257**, 277 (1960).

¹²W. B. Lewis, J. B. Mann, D. A. Liberman, and D. T. Croner, J. Chem. Phys. **53**, 809 (1970); and private communication.

¹³We are indebted to our colleague W. J. Childs who suggested this two-component model and carried out the detailed calculations.

¹⁴R. M. Sternheimer, Phys. Rev. **146**, 140 (1966).

¹⁵R. M. Sternheimer (private communication).

¹⁶I. Ahmad, H. Diamond, J. Milsted, J. Lerner, and R. K. Sjoblom, Nucl. Phys. A **208**, 287 (1973).

¹⁷S. G. Nilsson, Dan. Mat. Fys. Medd. **29**, No. 16 (1955).

¹⁸I. L. Lamm, Nucl. Phys. A **125**, 504 (1969).

¹⁹Z. Bochnacki and S. Ogaza, Nucl. Phys. **69**, 186 (1965).

²⁰N. Edelstein, J. Chem. Phys. **54**, 2488 (1971).

²¹A. J. Soinski, R. B. Frankel, Q. O. Navaro, and D. A. Shirley, Phys. Rev. C **2**, 2379 (1970).

²²J. L. C. Ford, Jr., P. H. Stelson, C. E. Bemis, Jr., F. K. McGowen, R. L. Robinson, and W. T. Milner, Phys. Rev. Lett. **27**, 1232 (1971).

²³K. E. Lobner, M. Vetter, and V. Honig, Nucl. Data Tables A **7**, 495 (1970).

²⁴W. N. Hooke, Phys. Rev. **115**, 453 (1959).

²⁵E. Browne and F. R. Femenia, Nucl. Data Tables **10**, 81 (1971).

²⁶M. W. Chen (private communication).

²⁷W. B. Lewis (private communication).